Long-wave infrared imaging for non-invasive beehive population assessment

Joseph A. Shaw,[1,*] Paul W. Nugent,[1] Jennifer Johnson,[1] Jerry J. Bromenshenk,[2,3] Colin B. Henderson,[2,3] and Scott Debnam[3]

[1]*Department of Electrical and Computer Engineering, Montana State University, Bozeman, Montana 59717, USA*
[2]*Division of Biological Sciences, University of Montana, Missoula, Montana 59812, USA*
[3]*Bee Alert Technology, Inc., 1620 Rodger St., Suite #1, Missoula, Montana 59802, USA*
**jshaw@montana.edu*

Abstract: Long-wave infrared imaging is used for non-invasive assessment of the internal population of honey bee colonies. The radiometrically calibrated camera signal is related to the number of frames that are populated by bees inside each hive. This enables rapid measurement of population without opening the hive, which disturbs the bees and can endanger the queen. The best results are obtained just before sunrise, when there is maximum thermal contrast between the hive and the background. This technique can be important for bee hive monitoring or for applications requiring frequent hive assessment, such as the use of bees for detecting chemicals or explosives.

OCIS codes: (110.3080) Infrared imaging; (110.6820) Thermal imaging; (120.0280) Remote sensing and sensors; (280.4991) Passive remote sensing; (280.1415) Biological sensing and sensors; (120.5630) Radiometry.

References and links

1. J. J. Bromenshenk, C. B. Henderson, and G. C. Smith, Biological Systems, paper II," in Alternatives for landmine detection (Rand Corp., 2003), *http://www.rand.org/publications/MR/MR1608/MR1608.apps.pdf*.
2. P. J. Rodacy, S. F. A. Bender, J. J. Bromenshenk, C. B. Henderson, and G. Bender, "The training and deployment of honeybees to detect explosives and other agents of harm," Proc. SPIE **4742**, 474–481 (2002).
3. L. Blazyte-Cereskiene, and V. Buda, "Ability of honey bees to detect and recognize isomers of cresol," Ekologija **53**(3), 16–21 (2007).
4. J. J. Bromenshenk, C. B. Henderson, R. A. Seccomb, S. D. Rice, R. T. Etter, S. F. A. Bender, P. J. Rodacy, J. A. Shaw, N. L. Seldomridge, L. H. Spangler, and J. J. Wilson, "Can honey bees assist in area reduction and landmine detection?" J. Mine Action **7.3** (2003), http://www.maic.jmu.edu/journal/7.3/focus/bromenshenk/bromenshenk.htm.
5. J. A. Shaw, N. L. Seldomridge, D. D. Dunkle, P. W. Nugent, L. H. Spangler, J. J. Bromenshenk, C. B. Henderson, J. H. Churnside, and J. J. Wilson, "Polarization lidar measurements of honey bees in flight for locating land mines," Opt. Express **13**(15), 5853–5863 (2005), http://www.opticsinfobase.org/oe/abstract.cfm?URI=oe-13-15-5853.
6. K. S. Repasky, J. A. Shaw, R. S. Scheppele, C. Melton, J. L. Carsten, and L. H. Spangler, "Optical detection of honeybees by use of wing-beat modulation of scattered laser light for locating explosives and land mines," Appl. Opt. **45**(8), 1839–1843 (2006), doi:10.1364/AO.45.001839.
7. D. S. Hoffman, A. R. Nehrir, K. S. Repasky, J. A. Shaw, and J. L. Carlsten, "Range-resolved optical detection of honeybees by use of wing-beat modulation of scattered light for locating land mines," Appl. Opt. **46**(15), 3007–3012 (2007), doi:10.1364/AO.46.003007.
8. J. J. Bromenshenk, C. B. Henderson, C. H. Wick, M. F. Stanford, A. W. Zulich, R. E. Jabbour, S. V. Deshpande, P. E. McCubbin, R. A. Seccomb, P. M. Welch, T. Williams, D. R. Firth, E. Skowronski, M. M. Lehmann, S. L. Bilimoria, J. Gress, K. W. Wanner, and R. A. Cramer, Jr., "Iridovirus and microsporidian linked to honey bee colony decline," PLoS ONE **5**(10), e13181 (2010).
9. J. D. Ellis, J. D. Evans, and J. Pettis, "Colony losses, managed colony population decline, and Colony Collapse Disorder in the United States," J. Apic. Res. **49**(1), 134–136 (2010).
10. R. M. Johnson, J. D. Evans, G. E. Robinson, and M. R. Berenbaum, "Changes in transcript abundance relating to colony collapse disorder in honey bees (*Apis mellifera*)," Proc. Natl. Acad. Sci. U.S.A. **106**(35), 14790–14795 (2009).
11. D. van Engelsdorp, J. D. Evans, C. Saegerman, C. Mullin, E. Haubruge, B. K. Nguyen, M. Frazier, J. Frazier, D. Cox-Foster, Y. Chen, R. Underwood, D. R. Tarpy, and J. S. Pettis, "Colony collapse disorder: a descriptive study," PLoS ONE **4**(8), e6481 (2009), doi: 10.1371/journal.pone.0006481.

#136135 - $15.00 USD Received 8 Oct 2010; revised 20 Dec 2010; accepted 20 Dec 2010; published 24 Dec 2010

12. J. A. Shaw, P. W. Nugent, N. J. Pust, B. Thurairajah, and K. Mizutani, "Radiometric cloud imaging with an uncooled microbolometer thermal infrared camera," Opt. Express **13**(15), 5807–5817 (2005), http://www.opticsinfobase.org/oe/abstract.cfm?URI=OPEX-13-15-5807.
13. P. W. Nugent, J. A. Shaw, and S. Piazzolla, "Infrared cloud imaging in support of Earth-space optical communication," Opt. Express **17**(10), 7862–7872 (2009), http://www.opticsinfobase.org/oe/abstract.cfm?URI=oe-17-10-7862.
14. A. Stabentheiner, and S. Schmaranzer, "Thermographic determination of body temperatures in honey bees and hornets: calibration and applications," Thermology **2**(4), 563–572 (1987).
15. B. Bujok, M. Kleinhenz, S. Fuchs, and J. Tautz, "Hot spots in the bee hive," Naturwissenschaften **89**(7), 299–301 (2002), doi:10.1007/s00114-002-0338-7.
16. M. Kleinhenz, B. Bujok, S. Fuchs, and J. Tautz, "Hot bees in empty broodnest cells: heating from within," J. Exp. Biol. **206**(23), 4217–4231 (2003).
17. A. Stabentheiner, H. Pressl, T. Papst, N. Hrassnigg, and K. Crailsheim, "Endothermic heat production in honeybee winter clusters," J. Exp. Biol. **206**(2), 353–358 (2003).
18. E. K. Es'kov, and V. A. Toboev, "Mathematical modeling of the temperature field distribution in insect winter clusters," Biophysics (Oxf.) **54**(1), 85–89 (2009).
19. M. Ono, T. Igarashi, E. Ohno, and M. Sasaki, "Unusual thermal defence by a honeybee against mass attack by hornets," Nature **377**(6547), 334–336 (1995).
20. G. Kastberger, and R. Stachl, "Infrared imaging technology and biological applications," Behav. Res. Methods Instrum. Comput. **35**(3), 429–439 (2003).
21. M. Greco, R. Spooner-Hart, and P. Holford, "A new technique for monitoring Trigona carbonaria nest contents, brood, and activity using X-ray computerized tomography," J. Apic. Res. **44**(3), 97–100 (2005).

1. Introduction

Honey bees have a strong sense of smell and can be conditioned to forage for buried land mines and explosives [1,2]. Such directed foraging can be fine tuned to isolate specific isomers [3]. We previously showed that it is feasible to use laser radar (LIDAR) to map out free-flying conditioned honey bees over a mine field to locate buried land mines [4,5]. The initial LIDAR experiment used a conventional direct-detection backscatter LIDAR instrument that could not distinguish between bees, vegetation, and other obstructions [5]. However, the small cross-polarized signal suggested that a significant fraction of the signal was caused by specular reflections from the bee wings. This led to the development of specialized LIDAR instruments that isolate bees from the near-static background through the detection of light modulated at the wing-beat frequency [6,7].

Along with the LIDAR for mapping bee concentrations in demining or explosive detection applications, operational deployment requires a need to maintain a large, robust, and potentially mobile bee population. Additionally, this must be done by personnel who lack the experience of a professional beekeeper. This suggests a need for a non-invasive method of estimating the size of the colony inside a set of hives with minimal time, labor, and cost. Such a method also would enable rapid and safe monitoring of the population of a large number of hives used in agricultural pollination. This is particularly timely, given the enormous losses to commercial bee populations in recent years as a result of Colony Collapse Disorder [8–11].

In this paper, we show the use of calibrated long-wave infrared cameras for non-invasive imaging of bee hive exteriors, with resulting radiance signals that are strongly correlated to the bee population in the hive. This method is enabled by new methods for generating and maintaining radiometric calibration of compact, microbolometer-based, long-wave infrared imagers for demanding scientific applications [12,13]. This technology provides previously unprecedented opportunities for thermal imaging in remote sensing applications where larger, more expensive, cryogenically cooled imagers are not practical. One such application is non-invasive monitoring of honey bee hives.

Infrared imaging has been used for several decades in specialized studies involving bee hives, but not for assessing hive population. For example, thermographically calibrated mid-wave infrared imagers have been used to study bee behavior inside hives fitted with infrared-transparent plastic panels in place of the normal wall material [14]. This general technique is being used to study the energetics and thermoregulation mechanisms that bees use to maintain their interior hive temperature, especially the brood nest, which is regulated to approximately 33-36°C [14–18]. Mid-wave infrared thermographic imaging also has been used to show that honey bees cluster in tight balls around an invading hornet, raising the temperature to

#136135 - $15.00 USD Received 8 Oct 2010; revised 20 Dec 2010; accepted 20 Dec 2010; published 24 Dec 2010

approximately 47°C, which is fatal to the hornet but not to the bees [19]. A wide variety of biological applications of infrared imaging have been reviewed [20], including the study of bee nest thermoregulation. The most detailed study of internal hive structure made use of X-ray computed tomography [21]. To our knowledge, we report the first application of non-invasive infrared imaging with unmodified hives to assess hive population.

2. Methodology

2.1 Infrared bee hive imaging

For this study we used a long-wave infrared camera with an uncooled microbolometer detector array of 324 × 256 pixels, responding over an optical bandwidth of 7.5-13.5 μm. The f/1.4 lens has 8.6-mm focal length, giving a field of view of 86° × 67°. Measurements were made with the camera located 3-4 m from the hives, so each hive was approximately 40 pixels wide. This is sufficient resolution to observe the spatial variation of hive radiance, as our algorithms do not retrieve detailed interior hive structure. The camera was calibrated with techniques we developed to track and compensate for changes in the camera response arising from changes in its temperature. The images have radiometric uncertainty of 0.5 W m^{-2} sr^{-1} when the camera is allowed to stabilize for at least 20 minutes before recording images. We sometimes used a large-area blackbody source alongside the hives to validate the calibration.

We recorded passive thermal images of dozens of hives multiple times in different weather conditions throughout both day and night. The measurements reported here were obtained in May 2010 before sunrise and after sunset with clear skies and calm air. The hives were located within a fence in an open field. The only nearby source of above-ambient radiance was a concrete utility shed located approximately six meters from the nearest hives. There were also two ambient-temperature sheds at similar distance from the hives (see Fig. 1).

The photograph in Fig. 1a shows six of the thirty-three hives included in this study. Each hive stack has one or more hive bodies; in this photograph, from left to right, there is a stack of four hive bodies, a stack of three bodies, and then four stacks of two bodies. Except for the half-sized bodies on the right-hand side of Fig. 1a, each body typically has room in its interior for ten honey frames (Fig. 1b). A manual inspection, conducted by opening the top and looking between frames, will find some frames to be populated by bees and some frames to be largely empty. In our analysis, we refer to "frame count" as the number of frames full of bees, rounded to the nearest integer for each hive body. In May 2010 during the measurements reported here, each frame contained approximately 5,000 bees.

Figure 2 shows a thermal image of the hives in Fig. 1, color coded to indicate band-integrated radiance (W m^{-2} sr^{-1}). Features to note include the following: 1) there are noticeable hot spots in the hives from bee-generated heat conducted through the hive wall and emitted from the hive; 2) the nearly empty narrow hive on the right-hand side shows no signature on its front, but does show elevated radiance on its side, which is either a reflection or re-emission from the adjacent hive; 3) the top hive body on the left-most stack has essentially no thermal signature because it is an empty hive body put in place the previous day to allow expansion of the large bee population; 4) the recessed handles emit more than the surrounding area, either because the body is thinner there or because of a cavity effect; 5) the warm object on the far right is a concrete building; 6) the ground in front of the hives has a patchy signature caused by patchy vegetation (before sunrise the vegetation is warmer than the surrounding soil and after sunrise the vegetation becomes cooler than the soil); 7) the clear sky emits a very low radiance (but clouds are much brighter and show up well when present) [12,13]; 8) the structure rising above the hives in the clear sky on the right is a power pole.

#136135 - $15.00 USD Received 8 Oct 2010; revised 20 Dec 2010; accepted 20 Dec 2010; published 24 Dec 2010

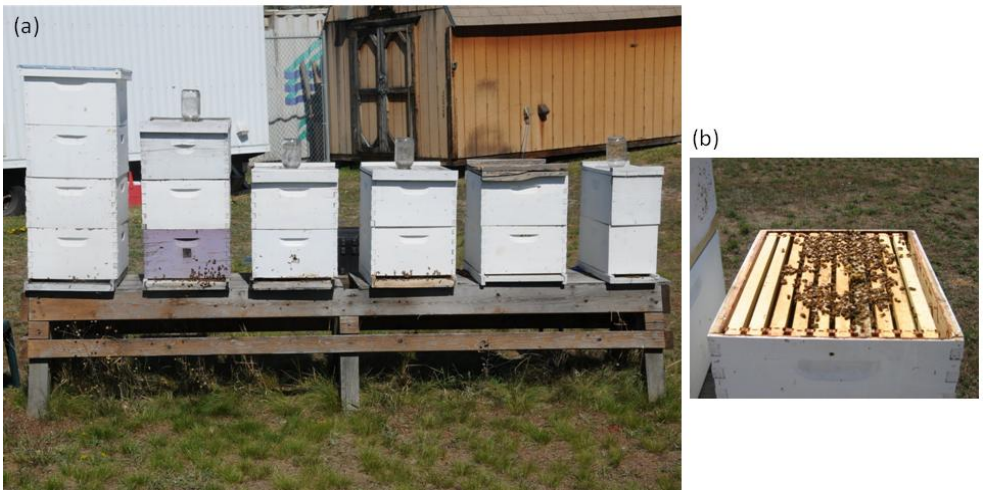

Fig. 1. Six of the thirty-three bee hives used in this study, showing stacks of (a) 4, 3, and 2 hive bodies and (b) ten frames inside one hive body with its top removed (the two left-most frames are without bees, so would not have been included in the frame counts used in the analysis.

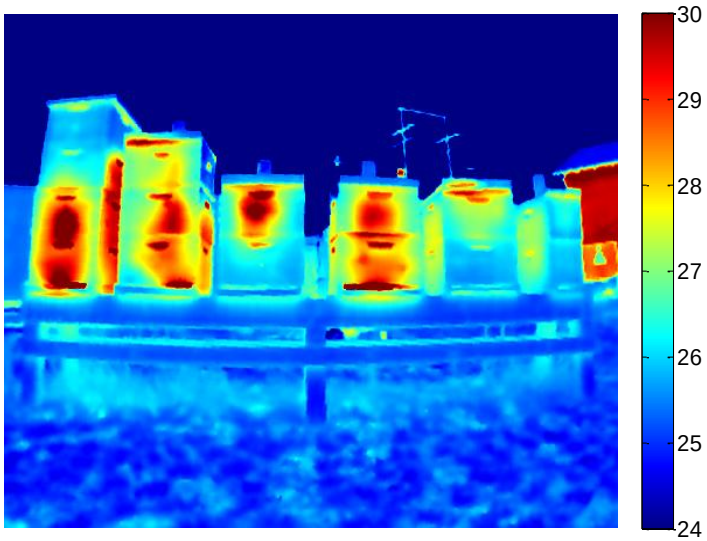

Fig. 2. (Media 1) Radiometrically calibrated long-wave infrared image of the bee hives shown in the visible photograph of Fig. 1, with the color bar indicating radiance (W m^{-2} sr^{-1}) Click the figure to play a time-lapse image sequence showing how the internal hive signature is overwhelmed by direct solar heating after sunrise at 6:30 AM (13 May 2010). With emissivity = 1, the radiance scale corresponds to temperatures of –12°C to 0°C; the air temperature was –4°C.

During multiple experiments we recorded thermal images during all hours of the day and night, finding the best thermal contrast between the hive signatures and the background in the morning just prior to sunrise. After sunrise, direct solar heating rapidly overwhelms the interior hive thermal signature.

Clicking on Fig. 2 activates a time-lapse infrared image sequence that shows the interior hive signature decaying in contrast after sunrise (local time is shown at the top of the images). The images were recorded once every thirty seconds and are displayed with 10 frames/s. The calculated apparent sunrise was at 6:04 AM, but because of the surrounding mountains direct sunlight did not hit the hives until approximately 6:30 AM. After 6:30, increasing sunlight

#136135 - $15.00 USD Received 8 Oct 2010; revised 20 Dec 2010; accepted 20 Dec 2010; published 24 Dec 2010

illuminates the scene and causes a shadow of a row of hives located behind the camera to move across the hives in these images. A metal shed in the background, seen on the far left-hand side of these images, is first illuminated by sunlight at 6:30, becomes noticeably brighter at 6:39, and greatly increases in radiance at 7:10 AM. The hive features that heat up the most rapidly are the purple-painted body at the bottom of the second stack from the left, the peeling-white-paint body at the top of the second stack from the left, and the metal top on the fifth hive stack from the left. The unpainted wooden bench on which the hives sit also heats up rapidly when illuminated by direct sunlight.

All colors of paint (and bare wood) have high long-wave infrared emissivity (typically greater than 0.9), so all hive paints, including white, are quite "black" in the long-wave infrared. Nevertheless, the higher short-wavelength absorption results in the purple-painted hive body at the bottom of the second hive from the left to experience much more rapid solar heating than the white hive bodies. There is similar rapid heating of the top hive body in the second stack from the left, as well as the unpainted hive table, which indicates the importance of well-maintained white paint for hive thermal regulation.

2.2 Image processing

After the hive images were calibrated radiometrically, the front (or back) face of an entire hive stack was selected using custom software that would calculate the radiance of the selected area. Care was taken to select the entire hive front (or back) without including the background, hive sides, or hive tops (which varied because of differing materials). From each thermal image, the software calculated the mean, minimum, maximum, and spatial standard deviation of the radiance. Additionally, a section of the image background was selected for determining hive-background contrast. The selected "background" typically was the grass in front of the hive table. Other background references were tested, including a large-area blackbody calibration source, an empty hive body, pieces of wood, and so forth. However, the technique worked as well without these specialized references, so in the interest of simplicity we adopted the approach of using the ground as a convenient reference. Nevertheless, care must be taken to consider current conditions, such as dew on vegetation.

When we imaged the hive fronts, the entrance region was selected separately from the total hive to prevent the typically warm entrance region from skewing the radiance values. Once the radiance values were calculated for each hive, we plotted the mean hive radiance, the difference between the maximum and minimum hive radiance, the difference between the mean hive radiance and the mean background radiance, and the hive radiance spatial standard deviation versus the normalized hive frame count (i.e., the number of bee-filled frames inside each hive body, divided by the number of bodies in the hive stack). We also tried plotting radiance statistics vs. the non-normalized frame count for each individual hive body, but thermal transfer between hive bodies in the same stack caused wide scatter in the results. Notice also that, although the results are reported as a normalized hive frame count through correlations with visual inspections, the results potentially could be reported in terms of estimated bee weight or number of bees.

A second method used to process the hive image data was an adaptive threshold-based approach. The hive images were de-skewed and re-sampled so that each hive body contained 100 × 100 pixels (approximately twice the native image resolution). An adaptive threshold based on the air temperature was applied to the hive and the number of pixels above threshold was determined. The relationship between the number of pixels above a correctly determined radiance threshold was found to be highly correlated with the population of the bee hives. This method also completely removes the dependence on the reference background radiance.

3. Results

In this section we plot the radiance statistics from thermal images recorded at the University of Montana bee yard in Missoula, Montana (46.84°N, 114.05°W) before sunrise on the morning of 13 May 2010. At the end of this section we show results of a modified data analysis method that reduces the dependence of the results on ambient air temperature.

#136135 - $15.00 USD Received 8 Oct 2010; revised 20 Dec 2010; accepted 20 Dec 2010; published 24 Dec 2010

Figure 3 contains four plots of radiance products plotted vs. normalized frame count. These plots show: (a) the mean radiance across the entire hive stack (front or back, depending on the direction of the camera relative to the hive); (b) the mean hive radiance minus the mean background radiance; (c) the maximum radiance from the hive front (or back) minus the minimum radiance for the same area; (d) the spatial standard deviation of the radiance across the hive front (or back). The data are plotted with red squares for the hive fronts and with blue diamonds for the hive backs. On each plot, the solid line is a linear fit to the hive-back data, and the dashed line is a linear fit to the hive-front data. The strongest correlations are for the mean radiance and mean-minus-background radiance plots, which show no significant difference between hive fronts and backs. The correlation is weaker for the max-min and standard deviation data, which also exhibit a slightly stronger correlation for the hive backs.

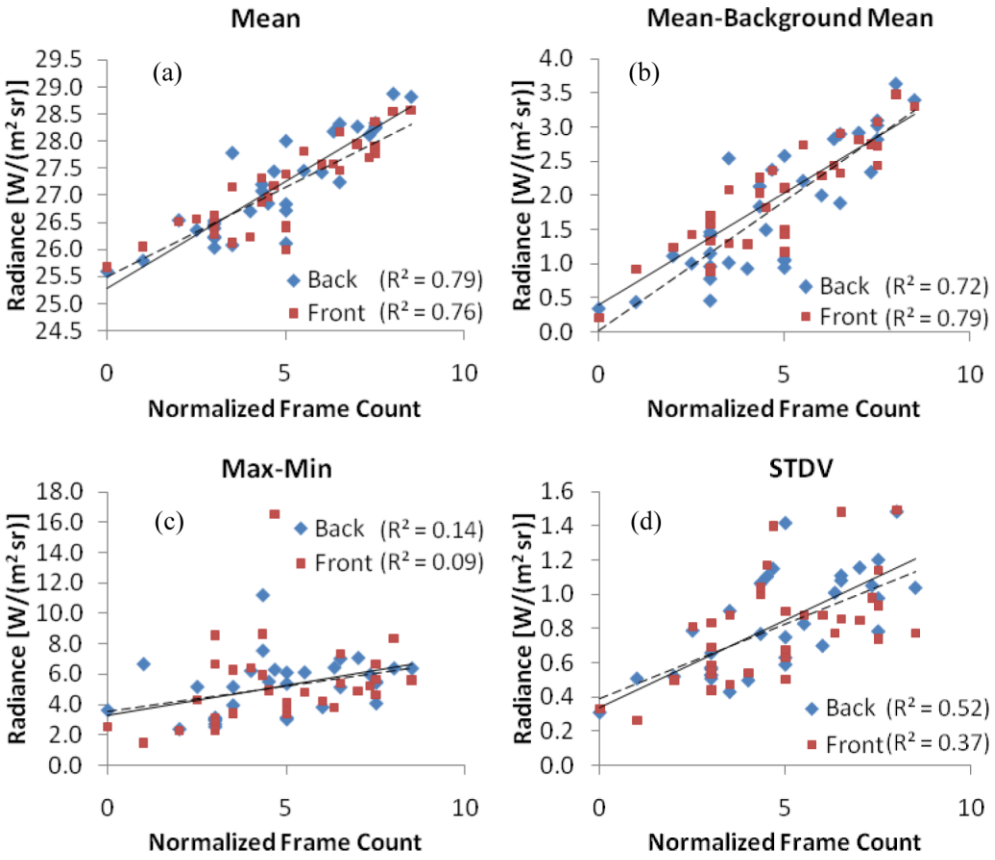

Fig. 3. Processed results for the 33 hives measured on the morning of 13 May 2010, plotted vs. normalized frame count (number of bee-filled frames in each hive stack, divided by the number of bodies in the stack): (a) mean hive back or front radiance; (b) mean hive back or front radiance minus the mean background radiance; (c) maximum radiance minus the minimum radiance; (d) standard deviation of the radiance across the hive back or front.

Figure 4 is a plot of the mean hive radiance vs. normalized frame count for images recorded approximately two hours after sunset on 12 May 2010 (compare with Fig. 3a). In this case, the linear fits to both hive-front and hive-back data have the same R^2 value, but the hive-back data are biased upward by approximately 0.5 W m^{-2} sr^{-1}. This is a result of the sun shining on the west-facing hive back during the afternoon before the sun set. We found that the method works reasonably well after sunset, but it was most consistent just before sunrise.

Because we nearly always see an elevated radiance at the entrance of hives with significant bee population, we explored the possibility of using the hive-entrance radiance alone as an indicator. The results are shown in Fig. 5 as a plot of hive-entrance radiance vs.

#136135 - $15.00 USD Received 8 Oct 2010; revised 20 Dec 2010; accepted 20 Dec 2010; published 24 Dec 2010

normalized frame count. The correlation is weaker than that for the entire-hive mean radiance and mean-minus-background radiance, but significantly stronger than that for the max-min and spatial standard deviation. This suggests that a simple measurement of the hive-entrance radiance may be a sufficient indicator of hive population.

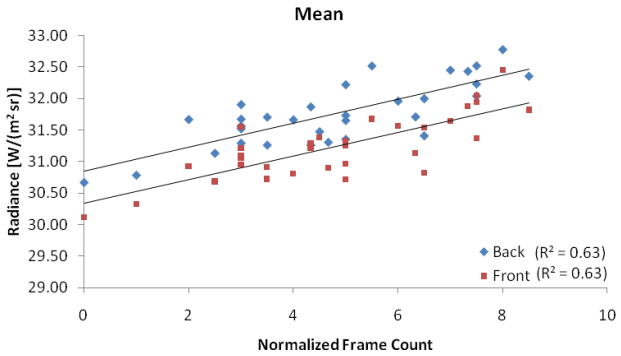

Fig. 4. Mean radiance of the hive backs (blue diamonds) and fronts (red squares) measured approximately two hours after sunset on 12 May, showing a back-front asymmetry resulting from the sun shining on the west-facing hive back later in the afternoon.

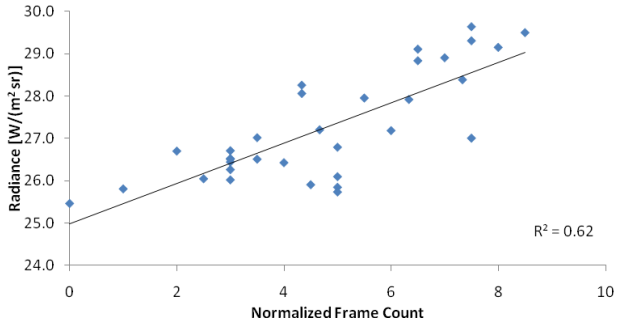

Fig. 5. Mean radiance for the hive entrances, plotted vs. normalized frame count (13 May am).

By comparing data from different times, it became apparent that the strong linear relationship between mean radiance and normalized frame count tends to always be present, with similar slopes but different offsets. This is illustrated in Fig. 6(a) as a plot of mean hive-front radiance for three measurement periods (12 May AM, 12 May PM, and 13 May AM). Recognizing that this may be related to the temperature difference between hive and the ambient air, we plotted in Fig. 6(b) the difference of mean hive-front radiance and the spectral band-integrated blackbody radiance at the air temperature (the air temperatures were 0.5°C for 12 May AM, 6.4°C for 12 May PM, and −4°C for 13 May AM). In this plot the lines for the morning data sets are brought closer together, but the evening one is still different. Therefore, we explored methods that might reduce the dependence on ambient air temperature.

To reduce the dependence on air temperature and background radiance, we also developed an algorithm that uses a radiance threshold that varies with the air temperature. The number of above-threshold pixels is used to determine the bee colony population, similar to how we identify and classify clouds in thermal infrared sky images [12,13]. In the bee hive algorithm, the hive images are de-skewed and re-sampled to 100 × 100 pixels per hive body to reduce the dependence on observation angle and distance from the hive.

#136135 - $15.00 USD Received 8 Oct 2010; revised 20 Dec 2010; accepted 20 Dec 2010; published 24 Dec 2010

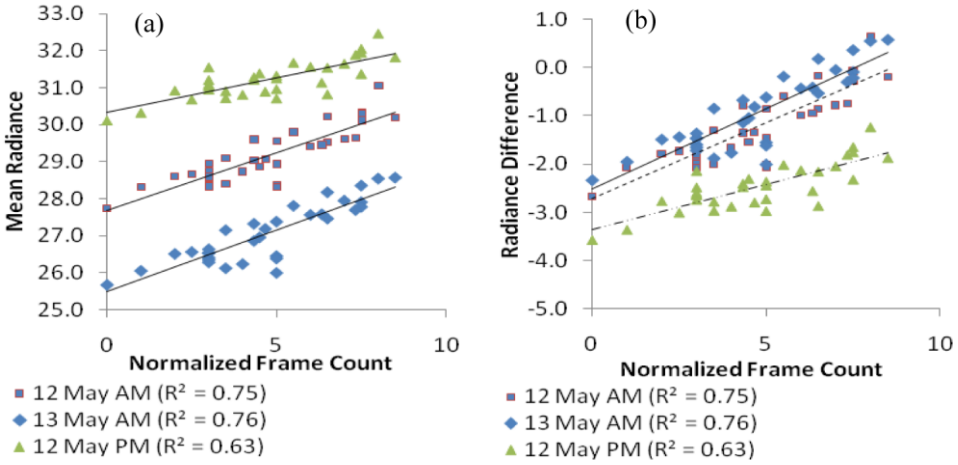

Fig. 6. Hive-radiance data for 12 May AM, 12 May PM, and 13 May AM: (a) mean radiance and (b) Mean radiance minus blackbody radiance at the ambient air temperature.

We used an iterative method to find the optimal threshold for each situation. Using an assumed threshold, the R^2 value was determined for a linear fit of the number of pixels above threshold and the total hive frame count. The threshold was varied in steps of 0.01, from 24 to 34 W m^{-2} sr^{-1}. Figure 7 (a) shows the R^2 values calculated for the hive fronts and backs over this range of thresholds. The optimal threshold for each data set was selected as the one that gave the highest R^2 value for both the front and back of the hives. The resulting optimal radiance thresholds are 28.5, 30.8, and 26.7 W m^{-2} sr^{-1} for the measurements from 12 May AM (air temperature = 0.5 °C), 12 May PM (air temperature = 6.4 °C), and 13 May AM (air temperature = –4.0 °C), respectively. These thresholds are plotted vs. blackbody radiance at the air temperature in Fig. 7 (b). This shows a strong linear relationship that can be used to predict the optimal threshold based on ambient air temperature; however, this relationship is expected to depend on the thickness of hive walls, spectral bandpass of the camera, etc., so users of this technique need to develop their own optimum-threshold relationship.

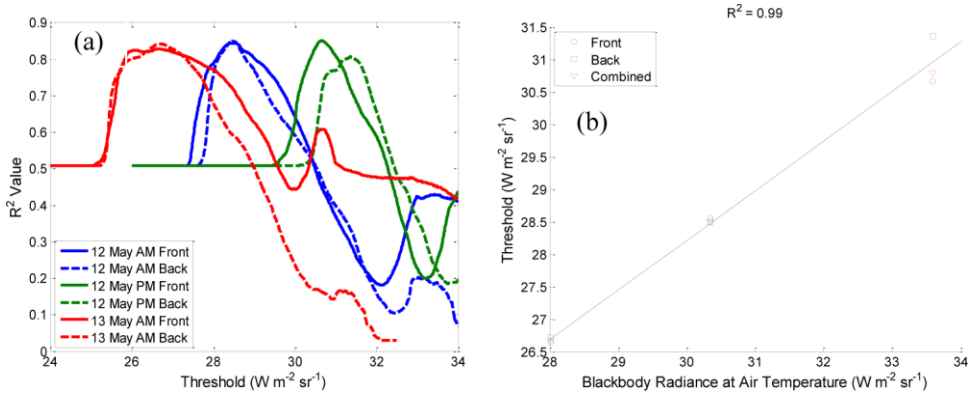

Fig. 7. Plots used to determine optimum threshold: (a) R^2 values for linear fits of above-threshold pixel count with frame count; (b) resulting relationship that can be used to determine the optimum threshold from ambient air temperature.

Figures 8 and 9 show the results of hive images processed with the threshold method. Figure 8 shows two pairs of hive images; each pair has a de-skewed and re-sampled hive image on the left and a thresholded hive image on the right with above-threshold pixels plotted in black. The hive-image pair shown on the left (C122) is a three-body hive that was nearly empty and had an above-threshold pixel count of 254 pixels (average of front and back

#136135 - $15.00 USD Received 8 Oct 2010; revised 20 Dec 2010; accepted 20 Dec 2010; published 24 Dec 2010

pixel counts). The hive-image pair shown on the right (C102) is a moderately full three-body hive, which had a frame count of 13 and an above-threshold pixel count of 19,755.

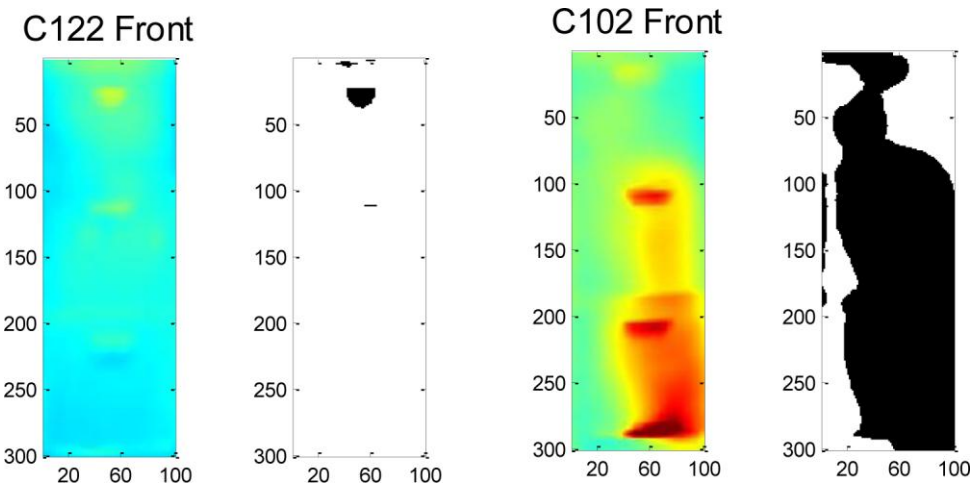

Fig. 8. Two image pairs are shown, each with a de-skewed and re-sampled thermal image on the left and the corresponding thresholded hive image on the right.

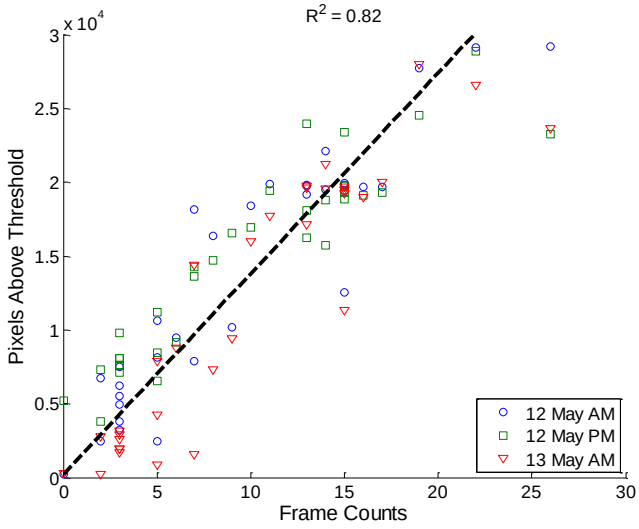

Fig. 9. Above-threshold pixel count (average of hive fronts and backs) plotted vs. frame count.

Figure 9 shows the number of pixels above threshold plotted vs. frame count for all three measurement periods. Unlike Fig. 7(a), these data all lie close to a common line, with a combined R^2 value of 0.82. The difference between the predicted and actual frame counts was ± 2.8 frames of bees (uncertainty in the visual inspections can be approximated at ± 2 frames of bees per hive body). Note that the maximum pixel count for a re-sampled image of a three-body hive is 3×10^4 and the maximum frame count is 30, but the data in Fig. 9 approach the maximum pixel count for a frame count near 22. This suggests that the present thresholds would result in a loss of sensitivity at the high end if the hive bodies were all full (the hives we used are managed to avoid totally full bodies). However, the two furthest outliers in Fig. 9, the 12 May PM and 13 May AM measurements with frame count near 25, are for a hive stack to which an empty hive body was added during the day of 12 May. The poor thermal sealing

#136135 - $15.00 USD Received 8 Oct 2010; revised 20 Dec 2010; accepted 20 Dec 2010; published 24 Dec 2010

and the hive disruption may both partly explain the changed thermal signature of this hive (we have seen thermal signatures remain disrupted 12 hours after a hive was opened).

4. Discussion and conclusions

The key result of this study is the demonstration that long-wave thermal imaging can be used for non-invasive assessment of the colony size inside a bee hive. This has great promise for both specialized applications of bees, such as demining and explosive detection, and widespread applications of bees, such as agricultural pollination and honey production. Thermal imaging reduces the time and labor, and therefore cost, required for monitoring hive populations.

The best results have been obtained from measurements made just before sunrise with clear skies and calm air. During the day, direct solar heating causes the thermal signature emanating from the hive interior to become difficult or impossible to measure. Quantitative assessment of the influence of nearby objects, trees, and sky conditions will require additional controlled experiments.

A method is presented that allows robust determination of the hive frame count from a count of pixels that are radiometrically greater than a pre-determined optimal threshold. If this relationship can be shown to remain constant over some reasonable length of time, this method will enable a user to rapidly perform non-invasive assessments after an initial experiment involving manual inspections to develop the relationship unique to the hives and camera used in the analysis. It is at least apparent from our analysis that slightly different optimal thresholds are found for hives with different wall thicknesses or levels of hive sealing.

An operational consideration is the distance from the camera to the hives. We conducted our measurements with the camera located approximately 3-5 m from the hives. Maintaining a relatively constant camera distance from the hives can help reduce the influence of atmospheric path emission (which increases rapidly with atmospheric water vapor content) and reduce uncertainties that may arise from vastly different pixel resolutions.

The methods presented here work well for the short study period included in this analysis. One of the key recommendations for future work is to perform a similar analysis over a longer time period and under a wider range of conditions. It will be particularly useful to investigate the feasibility of using these methods for monitoring wintering bee hives.

Acknowledgment

This work was supported by the U.S. Army RDECOM CERDEC Night Vision and Electronic Sensors Directorate (NVESD) through the contract W909MY-06-C-0037.

#136135 - $15.00 USD Received 8 Oct 2010; revised 20 Dec 2010; accepted 20 Dec 2010; published 24 Dec 2010